A 158 MHz RF ACCELERATING SYSTEM FOR COMPACT ELECTRON STORAGE RING "NIJI-1"

Hiroshi Takada and Yasumitsu Tsutsui
Osaka Research Laboratories, Sumitomo Electric Industries, Ltd.
Shimaya, Konohana, Osaka 554, Japan

Takio Tomimasu
Electrotechnical Laboratory
Sakura, Niihari, Ibaraki 305, Japan

ABSTRACT

A 158 MHz RF accelerating system for a compact test ring "NIJI-1" has been built, tested and set into operation. The results of RF measurements and behavior in testing are summarized. Though longitudinal coupled-bunch instability was observed in the ring, destructive modes which lead to beam loss were not present.

INTRODUCTION

The NIJI-1 constructed is a compact test ring for low energy injection studies.[1] Fig.1 shows the plane view of the ring. The ring consists of eight bending magnets, with field index of 0.47, whose bending angle is 45° and bending radius is 0.7 m. Edge focussing has been used with an edge angle of 12°. The lattice order is $0/2\ Q_F B_D Q_D B_D Q_F\ 0/2$ and the circumference of the ring is approximately 13 m. A RF cavity made of copper - clad stainless steel plate is installed. Its frequency is 158.4 MHz, the 7th harmonic of the revolution frequency.

At present the maximum beam current of 344 mA is obtained at electron injection energy of 163 MeV. The 1/e lifetime is approximately 50 minutes. In this paper we will show our experimental results in testing the cavity and its behavior in the ring.

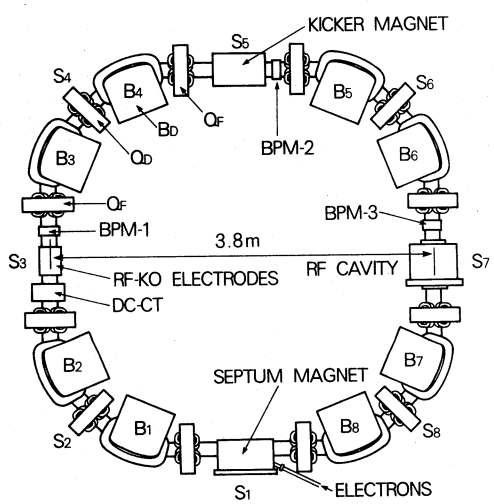

Fig. 1 Plane view of NIJI-1.

DESCRIPTION OF THE RF ACCELERATING SYSTEM

Fig.2 shows the re-entrant cavity for the ring. The cavity body and side flanges are mostly made of oxygen free copper-clad stainless steel plates. Accelerating electrodes and a tuning plunger are made of oxygen free copper. An acceleration gap between the electrodes of 180 mm and 115 mm in the outer and inner diameters is approximately 21 mm. With a change in position the tuning plunger with a 100 mm diameter can change the resonant frequency in the range of ±0.5 MHz by ±40 mm. The plunger is driven by a stepping motor. Electrical contacts between the electrodes and the side flanges are performed by Au-coated phosphor bronze contact spring setting in the groove of the electrode.

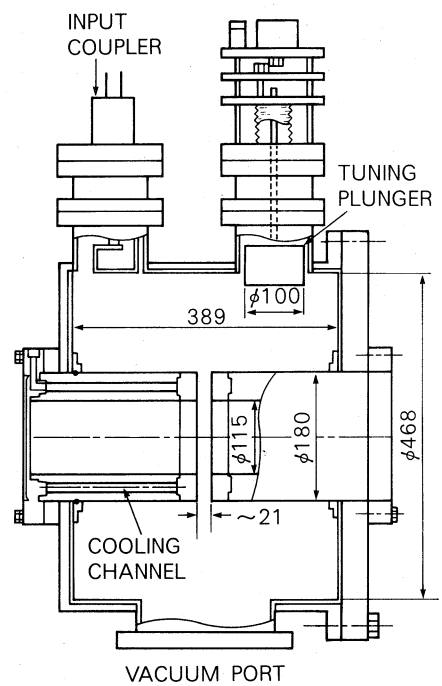

Fig. 2 Section of the cavity.

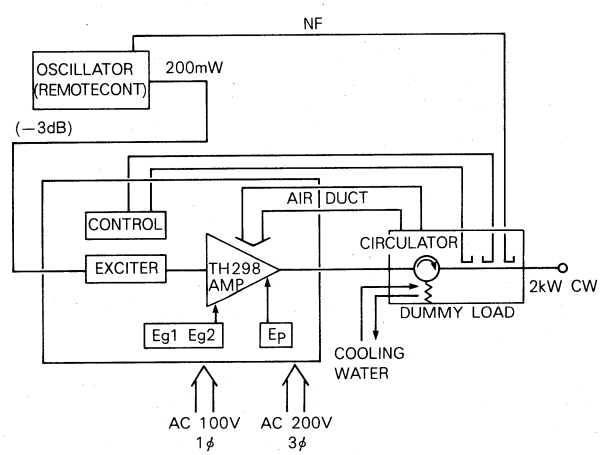

Fig. 3 Block diagram of the RF power generator.

A metal gasket between the body and one side of the flange enable it to keep both vacuum tightness and electrical contact. Water cooling channels are milled into the electrodes and the demountable flange. Semicircular water cooling tubes are welded outside the body and the opposite side flange-like structure. The cooling water is controlled in a temperature of 22°C with a ±1°C error range using a temperature regulation system.

An RF generator can excite the power up to 2 kW. A tetrode (TH298) is used for the amplifier. Fig.3 shows a block diagram of the RF power generator. The output RF power is supplied through a coaxial feeder of 1-5/8" EIA from the amplifier to the cavity. A ceramic vacuum window is adopted for use in the input coupler.

RF CHARACTERISTICS OF THE CAVITY

Resonant frequency and Q-value

A signal generator was connected to the cavity through a directional coupler; a network analyzer was connected to a sampling loop in the cavity. By varying the frequency of the signal generator, the resonance curve can be observed from whose bandwidth the loaded Q-value (Q_L) can be determined. Resonant frequency tuning was accomplished by changing the acceleration gap with several machinery cuts. The measurement showed that the acceleration gap dependence of the resonant frequency was 2.3 MHz/mm. The resonant frequency decreased by 0.2 MHz from an atmospheric state to a vacuum state. Finally, in the vacuum state after baking, the cavity operated satisfactorily in the required range of resonant frequency of 158.4 ± 0.5 MHz. The unloaded Q-value (Qo) is obtained by reducing the coupling coefficients sufficiently. Fig.4 shows the measured Q-values in atmospheric and vacuum states. The Qo is smaller than the calculated one by 40 ∿ 44 %. We think the difference between the measured and calculated values depends on the finishing conditions of the cavity inner surface and/or the installation of various kinds of ports.

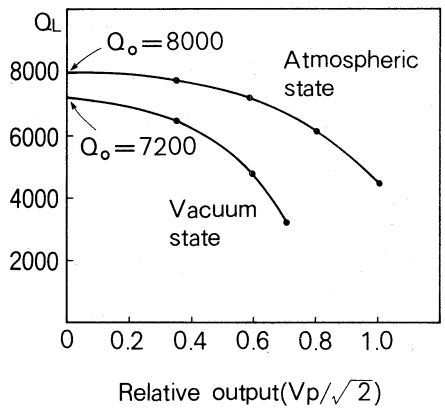

Fig. 4 Measured Q values.

Electric field distribution

Electric field E_z direction along the beam axis is measured by inserting a metallic bead which changes the resonant frequency of the cavity. The perturbation formula for TM_{010} mode is represented by

$$\Delta f = \frac{k\varepsilon E_z^2 \Delta\tau f}{2\int_{Vo}(\mu H^2+\varepsilon E^2)dVo.} \qquad (1)$$

Here Δf is the resonant frequency shift, k shape coefficient, $\Delta\tau$ bead volume and Vo cavity volume. For the measurement, the metallic bead 13.1 mm in diameter was attached to a thin cotton thread suspending it along the beam axis. The frequency shift due to the thread was extremely small, therefore it could be ignored when compared with measurement error. Fig.5 shows the relative magnitude of the electric field against the bead location. This electric field can produce the available beam acceleration.

Shunt impedance

Shunt impedance was measured using a perturbation technique. The value of Rsh/Qo for the TM_{010} mode is calculated from

$$Rsh/Qo = \frac{\{\int\sqrt{\Delta f/\Delta f_{max}}\,ds\}^2 \cdot \Delta f_{max}}{k\varepsilon\pi f^2 \Delta\tau}, \qquad (2)$$

here Δf_{max} is the maximum resonant frequency shift on beam axis. Although the shunt impedance is obtained from the bead volume $\Delta\tau \to 0$, the error of the measurement increases with the decrease of bead volume. Therefore, we used beads of 13.1 mm and 16.2 mm in

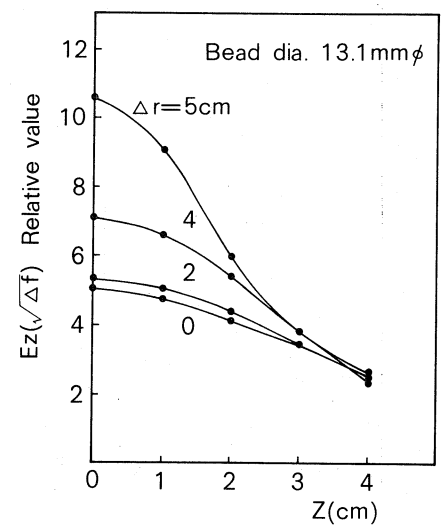

Fig. 5 Electric field distribution, Z is a distance from the acceleration gap center along the beam beam axis and Δr is a radial displacement from the beam axis.

diameter to determine the shunt impedance. The value was approximately 1.2 MΩ.

The value was also compared with the calculated value using the observed synchrotron frequency f_s and parameters of this ring in the present operation. The shunt impedance is given by

$$Rsh = \frac{V^2}{P - IUo}, \qquad (3)$$

$$f_s = \sqrt{\frac{\alpha h f_r^2 e V \cos\phi_s}{2\pi E}} \qquad (4)$$

Here α, h, fr, V, ϕs, E, P, I and Uo are the momentum compaction factor, harmonic number, revolution frequency, acceleration voltage, synchronous angle, electron energy, effective generator power, stored current and radiation loss, respectively. Substituting α=0.46, h=7, fr=22.6MHz, $\cos\phi_s \sim 1$, E=163MeV, p=0.7kW, I=100mA and U_0=0.083KeV, we obtain the shunt impedance of ∿1MΩ. Above measured value agrees approximately with the calculated value from Eqs.(3) and (4).

Input impedance

If the cavity does not match the amplifier under beam-loading, the RF is reflected from the cavity to the amplifier. However, it is possible to suppress the reflected power when input coupling coefficient β and tuning angle ψ are chosen in the range considered. In practice there is an upper limit of the reflected power by choosing β which equals to the power under no-beam and beam-loaded conditions.[2] The generator power for the acceleration voltage of V becomes

$$Pg = \frac{(1+\beta)^2}{4\beta}\frac{\{V+(IRsh/1+\beta)\cos\phi\}^2}{Rsh} \qquad (5)$$

The reflected power is

$$Pr = Pg - Pc - Pb, \qquad (6)$$

here Pc is the cavity dissipation $Pc=V^2/Rsh$, Pb the beam power, $Pb=IV\cos\phi=I \cdot U_0/e$ where Uo energy loss per turn.

In our ring, with Emax=230MeV, Imax=300mA, V=26kV, Rsh=1.2MΩ and U_0=0.35KeV, the calculated β and Pg are $\beta \sim 1$, $Pg \simeq 0.35$kW, respectively. Therefore, the input impedance of the cavity was matched to the characteristic impedance (50Ω) of the feeder with a network analyzer.

VACUUM CONDITION AND POWER TEST

After machining the electrodes for the adjustment of the resonant frequency and measurements of the characteristics exposed to air, the cavity inner surface was cleaned with etylalcohol and rinsed with freon 113. Vacuum was obtained 2.8×10^{-8} Torr by roughing with rotary and turbomolecular pumps; the pumping speeds of the rotary and turbomolecular pumps are 150 ℓt/min and 160 ℓt/s, respectively. A mass spectrum analyzer was used to check for leaks among the residual gas components. In Fig.6(a) is spectra relative to this situation. There were mainly H_2, some H_2O, CO and CO_2 without N_2 and O_2. After outgassing for 18 hours at ∿200°C the pressure reached 1.1×10^{-9} Torr by using a sputter ion pump with pumping speed of 500 ℓt/s and a titanium sublimation pump with 750 ℓt/s. Vacuum condition was good. The residual gas was dramatically reduced as shown in Fig.6(b).

We encountered difficulty in trying to feed RF power into the cavity for the first time. The phenomena could be explained by discharges between the acceleration gap as the multipacting voltage was calculated below 1.2 kV. After enough ageing, the RF power could be supplied. Fig.6(c) shows the residual gas components at a power of 0.5 kW. H_2O which isn't removed by baking and ageing is the highest peak. After a full power test, the cavity was installed in the ring.

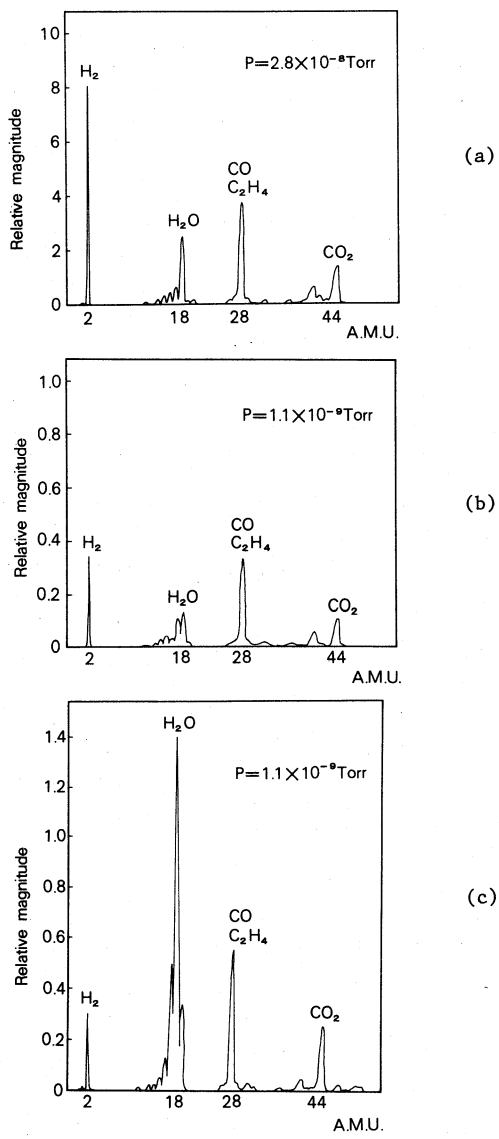

Fig. 6 Residual gas spectra, (a) without RF; P=2.8 $\times 10^{-8}$ Torr, (b) without RF; P=1.1 $\times 10^{-9}$ Torr (c) with RF of 0.5 kW; P=1.1 $\times 10^{-9}$ Torr.

BEAM INSTABILITY

Though the resonant frequency of 158.4 MHz is used for electron acceleration, the harmonics of the frequency exist in the cavity. We observed the frequency spectra of a signal from a sampling loop of the cavity with a spectrum analyzer. Fig.7 shows that the frequencies of the peaks coincide to the higher-order modes at no stored beam current and an RF power of 0.75 kW.

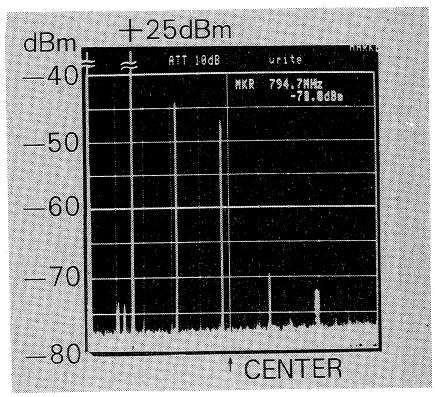

Fig. 7 Frequency spectrum of the transmitted power from the cavity at no stored beam current, 500 MHz center frequency, 200 MHz/div.

Since the cavity has the highest Q-value in a vacuum doughnut, the cavity is the most probable suspect that causes coupled-bunch instabilities. If the beam signal has other frequency components than the harmonics n of the resonant frequency, we can conclude that the instabilities are occuring in a ring. The signal spectrum consists of the frequencies

$$f^{\pm}_{\mu,n} = nhf_r \pm (\mu f_r + mf_s). \qquad (7)$$

Here fr is the revolution frequency, fs the synchrotron frequency, h harmonic number, μ mode number and m shape mode number. Frequencies $f_{\mu,n}$ are present with nearly symmetric sidebands as shown in the beam spectrum example in Fig.8. Although the enlargement of a beam size is recognized, modes which are destructive and lead to beam loss aren't observed in the present operation. The beam storage up to 340 mA has already been achieved. There is no indication that the maximum stored current is limited by coupled-bunch instabilities. The detailed studies of tune dependence, cooling temperature dependence and so on for beam instability are in progress.

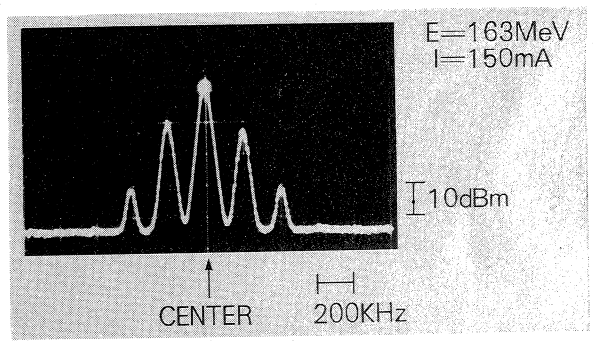

Fig. 8 Synchrotron frequency sidebands, 135.77 MHz center frequency (μ=1,6).

REFERENCES

1) H. Takada et al., Proc. SPIE, 773, pp.257-263 (1987)
2) M. Watanabe et al., UVSOR-9, pp.48 (1982)
3) E. Weihreter et al., IEEE Trans. Nucl. Sci., NS-32 pp.2317-2319 (1985)
4) H. Kobayakawa et al., Jpn. J. Appl. Phys. 26, pp.864-874 (1986)